PV POWER OUTPUT PREDICTION USING DEEP LEARNING

Thomas Lionel Makosso[1] , Ali Almaktoof[2] , Khaled Abo − Al − Ez[3]
[1] Cape Peninsula University of Technology (CPUT), Cape Town, South Africa
[2] Cape Peninsula University of Technology (CPUT), Cape Town, South Africa
[3] University of Johannesburg, Johannesburg, South Africa
*corresponding author's email: 218283695@mycput.ac.za

Abstract

Photovoltaic (PV) systems generate solar power worldwide. Solar power sources are unpredictable by nature because the output power of PV systems is alternating and heavily dependent on environmental conditions. Among these are wind speed, humidity, PV surface temperature, and irradiance. Planning ahead is essential for solar power generation due to the unpredictable nature of photovoltaic systems, much as forecasting solar electricity is necessary for the electric grid. The irradiance has a significant impact on solar power generation, making weather forecasting challenging and complex. There is discussion of how different environmental factors affect a photovoltaic system's output. In order to overcome the difficulties caused by the variability of solar radiation, this research explores the application of deep learning for photovoltaic (PV) power output prediction. The confusion matrix and ROC AUC results reveal that the proposed deep learning model predicted accurately the power output.

1. Introduction

Photovoltaic (PV) power generation is at the forefront of sustainable development due to the growing significance of renewable energy sources in mitigating climate change and guaranteeing energy security [1]. Solar power, when used with photovoltaic systems, is a clean, abundant energy source that has experienced significant growth and technological advancement [2]. The intrinsic fluctuations and sporadic nature of solar radiation present notable obstacles to the assimilation of photovoltaic power into the power system [3]. Precise forecasts of photovoltaic power output are essential for maximizing energy distribution system efficiency, strengthening grid stability, and optimizing energy management [4]. Because deep learning can extract intricate patterns from vast datasets, it has become a strong and adaptable technique for modeling and forecasting PV power output in this context [5]. Deep learning is a branch of machine learning that uses multi-layered artificial neural networks to automatically extract and change features from unprocessed data [6]. Because of this ability, deep learning is especially well-suited to managing the stochastic and nonlinear aspects of solar power generation, which are influenced by a variety of variables like the weather, one's location, and the time of day [7,8]. Deep learning models can capture complex interactions and dependencies within the data, which leads to more accurate and dependable forecasts than standard forecasting techniques, which frequently rely on handmade features and linear assumptions [9]. This study intends to increase renewable energy forecasting and aid in the shift to a more resilient and sustainable energy grid by utilizing deep learning for PV power production estimates and implement a variation of the irradiance for testing purposes. Researchers looking to maximize solar energy use and more successfully incorporate renewable resources into the power grid may find great value in the discoveries and approaches discussed here.

2. Methodology

The ANN approach, which is motivated by the way a neuron functions biologically, is used in this study to forecast the output power of a PV module[10]. In the same manner that a neuron in the human brain processes signals, a neural network processes the information (inputs and outputs) of a dynamical system, the mathematical modelling of which is a challenging undertaking. Its appeal is that it eliminates the need for extensive knowledge of the dynamical system, as obtaining data for that system is a laborious and intricate procedure.[11].

The function of neurons is necessary for the operation of ANNs. The training algorithm presented in figure 1 was developed in Python. Measurements of Voltage and Currents were taken from the PV and process through this algorithm

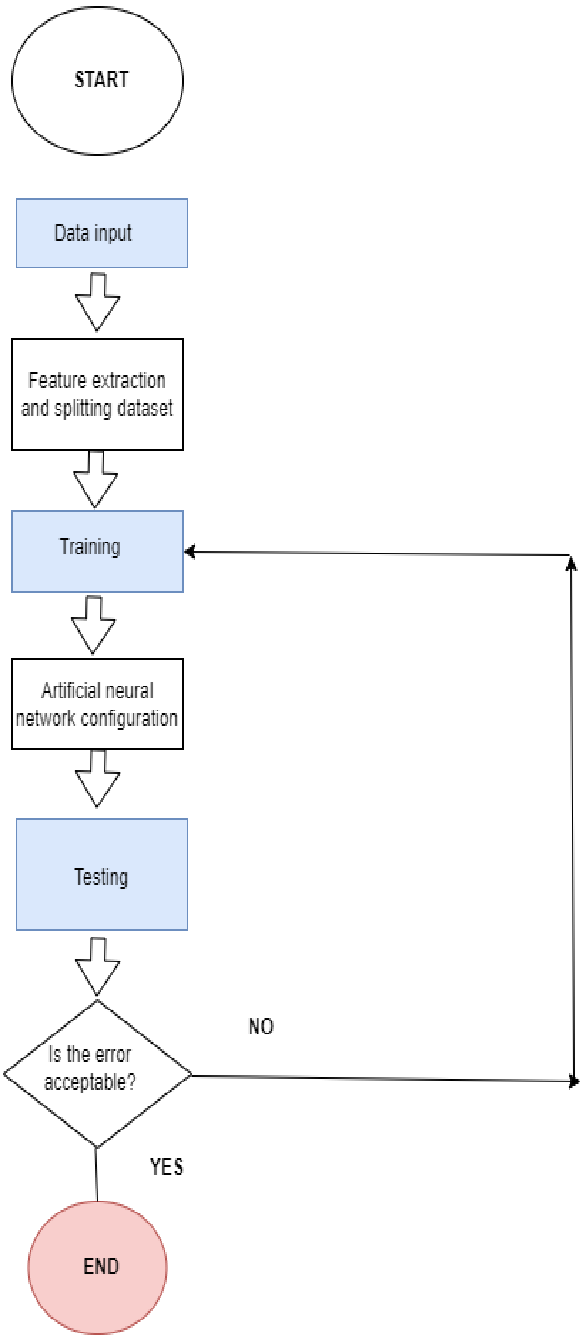

Figure 1: Training algorithm

3. Mathematical modelling of a PV

Numerous authors have successfully developed a number of PV models. In actuality, two models—the one with one diode and the one with two diodes—are the most often used(Tsioumpri 2020). The most common diode model is this one. Its electrical model is shown in Figure 9. The power output of the PV generator is calculated using:

$$I^{m/p} = I_{ph_{m/p}} - I_{o_{\frac{m}{p}}}\left[\exp\left(\frac{\left(V^{\frac{m}{p}} + R_{s_{\frac{m}{p}}} \times I^{\frac{m}{p}}\right)}{nV_{T_{\frac{m}{p}}}}\right) - 1\right] - \left(V^{\frac{m}{p}} + R_{s_{\frac{m}{p}}} \times I^{\frac{m}{p}}\right)/R_{p_{\frac{m}{p}}} \qquad (1)$$

$$I^{m/p} = I_{ph_{m/p}} - I_{o1_{\frac{m}{p}}}\left[\exp\left(\frac{\left(V^{\frac{m}{p}} + R_{s_{\frac{m}{p}}} \times I^{\frac{m}{p}}\right)}{n_1 V_{T_{\frac{m}{p}}}}\right) - 1\right] - \cdots I_{o2_{\frac{m}{p}}}\left[\exp\left(\frac{\left(V^{\frac{m}{p}} + R_{s_{\frac{m}{p}}} \times I^{\frac{m}{p}}\right)}{n_2 V_{T_{\frac{m}{p}}}}\right) - 1\right] - \left(V^{\frac{m}{p}} + R_{s_{\frac{m}{p}}} \times I^{\frac{m}{p}}\right)/R_{p_{\frac{m}{p}}} \qquad (2)$$

$$P^{m/p} = V^{m/p}.I^{m/p} \qquad (3)$$

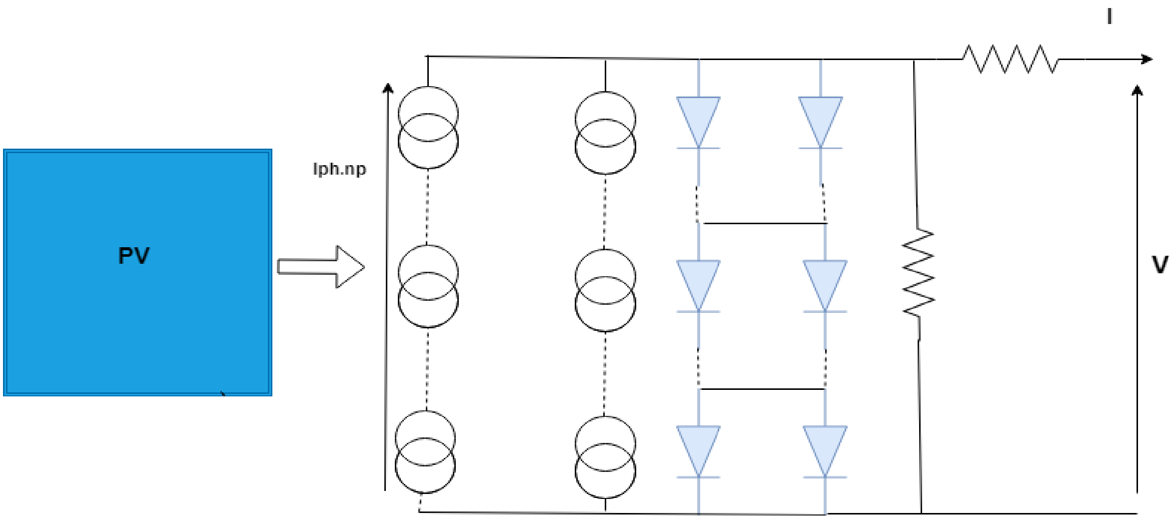

Figure 2: Electrical model

The combination of the saturation currents of the diodes and the inclusion of a single idealistic factor n serve as the inspiration for the idea of a diode model. It has been confirmed in recent years that the single-diode model can successfully adapt to some extent to experimental data[12]. This model's representation can be expressed as given in equation (2.1).
In the described equation there is 5 main parameters to determine the photocurrent $I_{ph_{m/p}}$, saturation current $I_{o_{\frac{m}{p}}}$, series and parallel resistance $R_{s_{\frac{m}{p}}}$ and $R_{p_{\frac{m}{p}}}$,coeffient of ideality n
The double diode model significantly increases the PV system's accuracy, but it requires more complicated parameter calculations(Huang and Kuo 2019). Regarding the single-diode model, it is much easier to use and is the most commonly used in literature(da Silva and Meneses 2023).
A PV system is made up by a set of cells mounted in parallel and series, which are described by the following equation:

$$I_{PV} = N_P . I_{phm} - N_P . I_{om}\left[\exp\left(\frac{V_{pvm} + I_{pvm} . R_{sm}\left(\frac{N_S}{N_P}\right)}{nN_S V_{Tm}}\right) - 1\right] - \frac{V_{pvm} + I_{pvm} . R_{sm}\left(\frac{N_S}{N_P}\right)}{R_{sm}\left(\frac{N_S}{N_P}\right)} \quad (4)$$

3.1 Relationship between the conditions of operation and the PV

The known and unknown parameters of the photovoltaic system model vary depending on the actual operating circumstances (light intensity and temperature), to which photovoltaic panels are most often subjected [13]. Therefore, it is essential to understand the relationships between the PV system's parameters and operating circumstances, particularly light intensity and temperature [14]. As a result, the extraction of parameters is dependent upon the meteorological conditions under which PV operations [15]. Figure 3 illustrates the relationship between the parameters and the PV

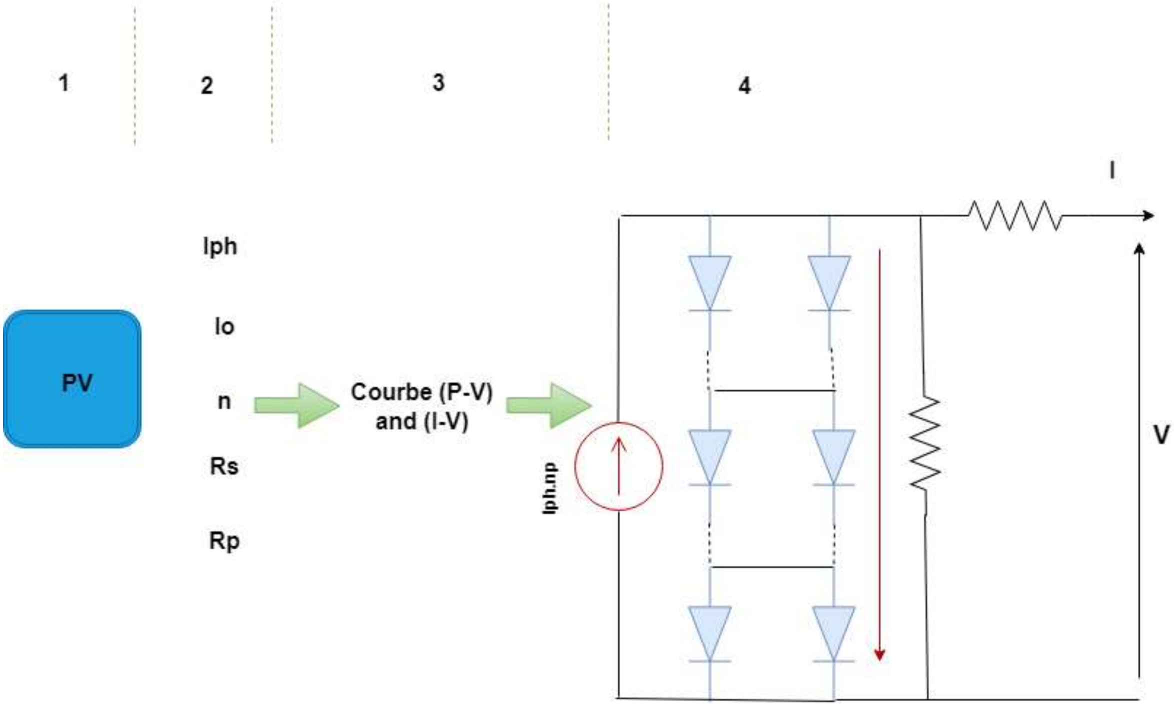

Figure 3: Relationship between the parameters and the PV

3.2 Standards conditions

The equation 1 can be reduced to:

$$I^{m/p} = \left(I_{ph_{m/p}}\right)_{ref} - \left(I_{0_{m/p}}\right)_{ref}\left[exp\left(\frac{\left(V^{\frac{m}{p}} + \left(R_{S_{m/p}}\right)_{ref} \times I^{\frac{m}{p}}\right)}{n\left(V_{T_{m/p}}\right)_{ref}}\right) - 1\right] - \left(V^{\frac{m}{p}} + \left(R_{S_{m/p}}\right)_{ref} \times I^{\frac{m}{p}}\right) / \left(R_{S_{m/p}}\right)_{ref} \quad (5)$$

The following equations can be established, respectively, based on the assessment of the currents at specific short circuit points:

$$\left(I^{m/p}\right)_{sc,ref} = \left(I_{ph_{m/p}}\right)_{ref} - \left(I_{0_{\frac{m}{p}}}\right)_{ref} \cdot \left[exp\left(\frac{\left(\left(R_{S_{m/p}}\right)_{ref} \times \left(I^{m/p}\right)_{sc,ref}\right)}{n\left(V_{T_{m/p}}\right)_{ref}}\right) - 1\right] - \left(\left(R_{S_{m/p}}\right)_{ref} \times \left(I^{m/p}\right)_{sc,ref}\right) / \left(R_{S_{m/p}}\right)_{ref}$$

$$\left(I_{ph_{m/p}}\right)_{ref} - \left(I_{0_{\frac{m}{p}}}\right)_{ref} \cdot \left[\exp\left(\frac{\left(\left(V^{m/p}\right)_{0ref}\right)}{n\left(V_{T_{m/p}}\right)_{ref}}\right) - 1\right] - \left(\left(V^{m/p}\right)_{0,ref}\right) / \left(R_{S_{m/p}}\right)_{ref} \qquad (6)$$

3.2.1 Under real conditions

Short circuit current $\left(I^{m/p}\right)_{sc,ref}$ is linked with and the photocurrent $\left(I_{ph_{m/p}}\right)_{ref}$ through the following equation:

$$\left(I^{m/p}\right)_{sc,ref} \approx \frac{\left(I_{ph_{m/p}}\right)_{ref}}{\left(1+\frac{\left(R_{S_{m/p}}\right)_{ref}}{\left(R_{P_{m/p}}\right)_{ref}}\right)} \qquad (7)$$

If the model is ideal $\left(I^{m/p}\right)_{sc,ref} \approx \left(I_{ph_{m/p}}\right)_{ref}$

$$R_p = R_{pref} \cdot \left(\frac{T}{T_{ref}}\right) \qquad (8)$$

Numerous values of n that are based on empirical analyses can be found in the literature. Other authors use the following relationship to determine the idealistic factor in test standards [16].

$$n_{ref} = \frac{q\left(2\left(V_{T_{m/p}}\right)_{ref} - V_{OC\,ref}\right)}{N_S KT\left(\ln\left(1-\frac{I_{mppref}}{I_{scref}}\right) - \frac{I_{mppref}}{I_{scref}-I_{mppref}}\right)} \qquad (9)$$

3.3 Characteristics of a PV module

These characteristics vary as a function of temperature, and irradiation leading to variation of curves (I-V) and (P-V) as a function of temperature and irradiation, as illustrated in Figure 4 which are the I-V Characteristics**.**

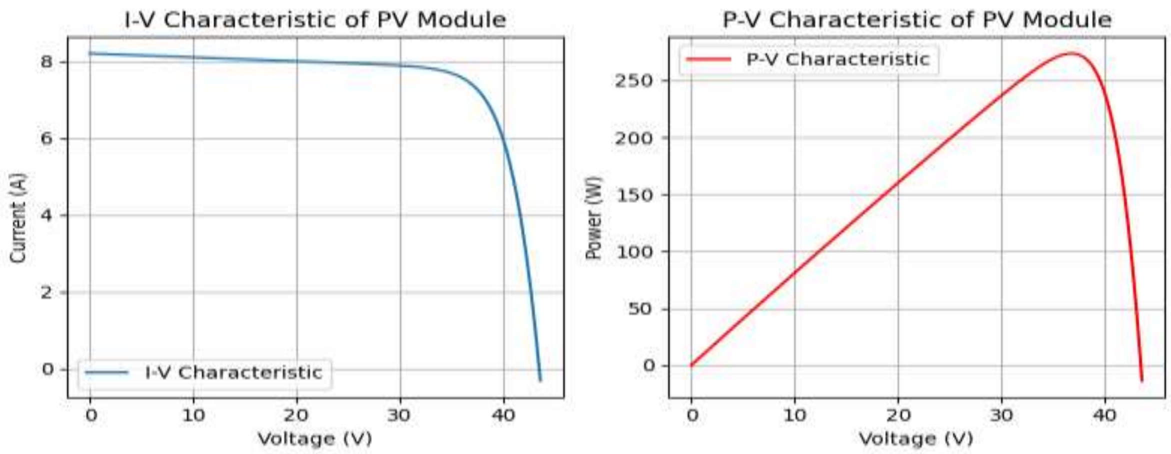

Figure 4: I-V Characteristics

4. Simulation results

In this section, we present the result obtained from two scenarios. The first scenario considers a steady irradiance of 1000 while the second one used a variable irradiance of 0 to 1000. The table 1 provides the details of the Parameters that were used in the model.

Table 1: Details of the Parameters

Parameters	Values
Number of epochs	1000
Metrics	Mean Square Error
Activation Function	Sigmoid
Input size	2
Output size	1
Hidden layer	4
Learning rate	0.1

4.1 Linear regression

The Figure 1 shows the algorithm computed in Python to develop the neural network. It is a backpropagation algorithm that compare the actual and the predicted values of the PV power

4.2 Scenario 1

The regression was used to demonstrate how much the predicted PV output matched with the actual value. In Figure 5 and 6 show respectively the Linear regression with steady irradiance and Power prediction case 1. It can be seen that the Predicted dots are closer to the ideal fit which means that the proposed neural network carried out perfectly the prediction purposes.

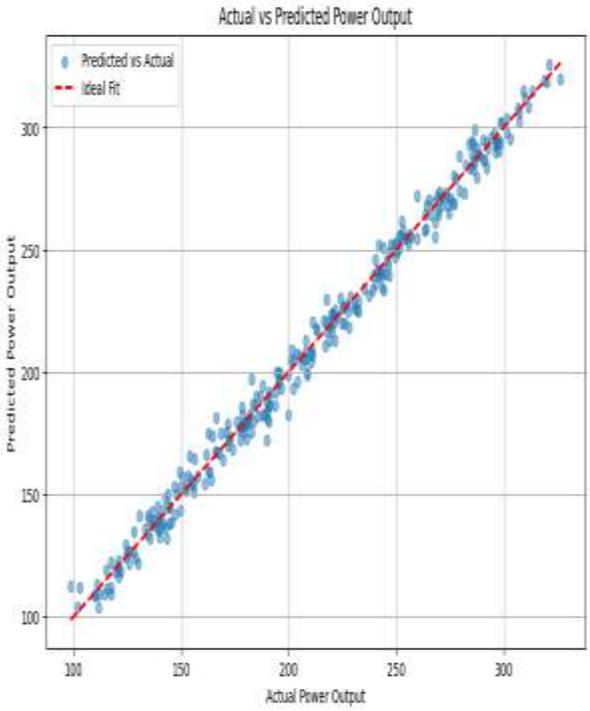

Figure 5: Linear regression with steady irradiance

	Actual Power Output	Predicted Power Output
521	211.138383	207.025088
737	296.473946	293.512644
740	228.641126	221.225031
660	204.533752	200.550905
411	313.342266	318.744968
678	330.342850	321.470819
626	215.397890	221.225031
513	307.405232	301.966289
859	137.804063	145.631612
136	236.797607	232.536849
811	283.172865	297.494941
76	280.092291	282.484523
636	236.808519	238.999147
973	163.834911	171.431864
938	157.097476	154.127956
899	144.943605	145.876697
280	311.859562	307.402981
883	147.782606	153.158736
761	201.205672	194.446349
319	181.781022	181.408497

Figure 6: Power prediction case 1

4.3 Scenario 2

In the second scenario, the irradiance was varied randomly from 500 to 1000. The same neural network model was used to predict the ideal output. In Figure 7 and 8 the Linear regression with varying irradiance Power prediction case 2 were presented. From the range of 100 to 300 it can be seen that the predicted value is close to the values of the actual power output.

In the process of the algorithm, the proposed model ran 1000 epochs and then printed 20 random epochs to analyse the gap between the Predicted and the actual results.

ISSN: 2633-4828 Vol. 6 No.4, December, 2024

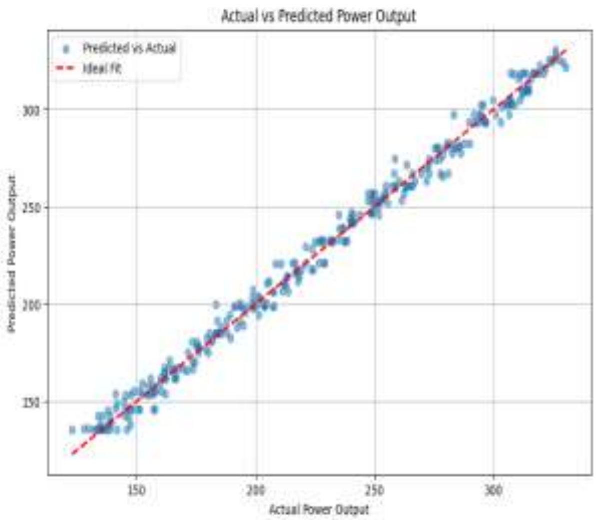

Figure 7: Linear regression with varying irradiance

	Actual Power Output	Predicted Power Output
521	205.197831	206.272010
737	276.270413	269.549652
740	217.788685	216.592418
660	193.648840	186.178640
411	296.596060	293.579105
678	295.676673	297.737720
626	208.652985	198.688003
513	270.845962	271.354270
859	142.686108	136.362810
136	230.710771	225.795525
811	296.274239	290.079962
76	266.123146	264.343866
636	216.356709	220.961005
973	160.943878	154.580975
938	138.428698	136.905414
899	136.456349	143.150871
280	301.311424	298.080505
883	141.807728	143.631707
761	190.163841	180.711650
319	150.784537	156.912613

Figure 8: Power prediction case 2

4.4 Performance analysis

Interpreting the ROC AUC and confusion matrix findings can provide a thorough understanding of a classification model's performance. The model's capacity to discriminate between classes is measured by the ROC AUC (Receiver Operating Characteristic - Area Under the Curve).

, in this study those metrics were used for a regression model. Figure 9 and 10 presents respectively the ROC AUC performance case 1 and case 2 performance metrics evaluation in the first and second scenario. Looking at the ROC in both cases the model obtained a value between 0.9 and 1 in all the three classes which means that the regression model work as expected.

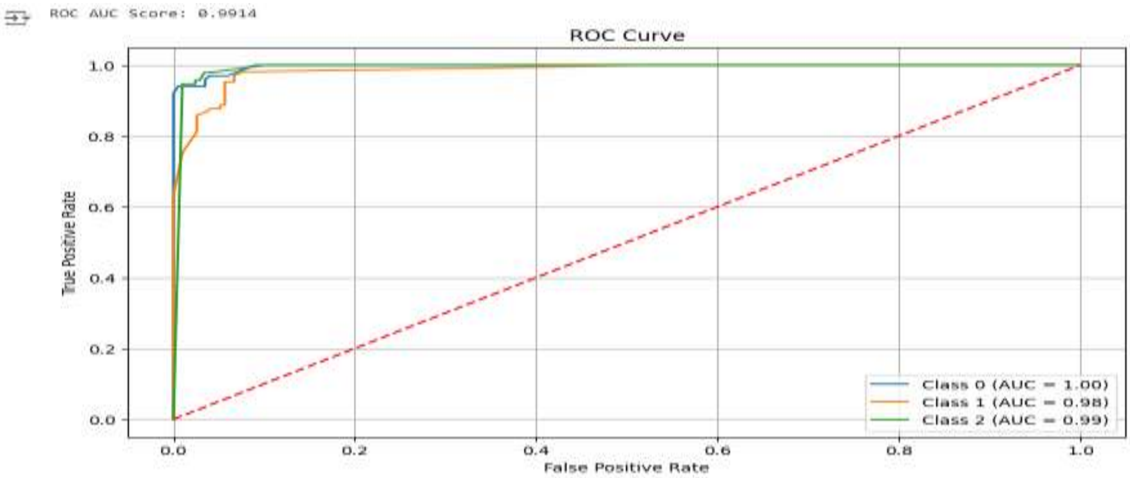

Figure 9: ROC AUC performance case 1

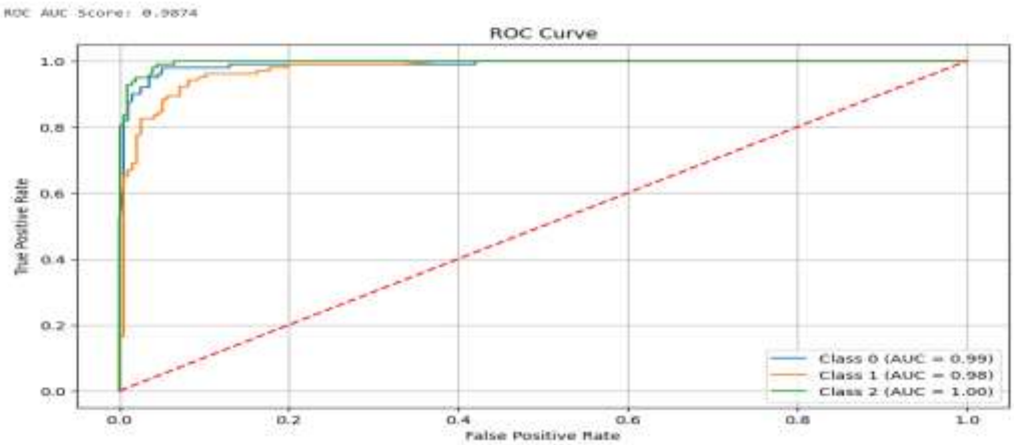

Figure 10: ROC AUC performance case 2

Conversely, the confusion matrix offers a comprehensive understanding of the model's predictions. True Positives (TP), True Negatives (TN), False Positives (FP), and False Negatives (FN) are its four constituent parts. The Figure shows respectively the Confusion Matrix in Scenario 1 and 2. The diagonal represents the number of true positives which are the scenario that predicted accurately the power output. So in most three classes, there no predictions errors that exceeds 9, it is between 0 and 5 while there is a high number of correct predictions almost 276.

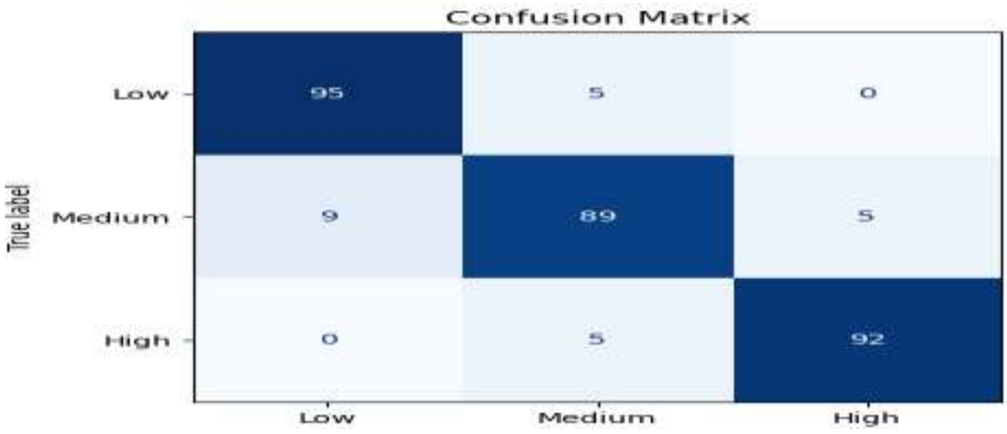

Figure 11 : Confusion Matrix in Scenario 1

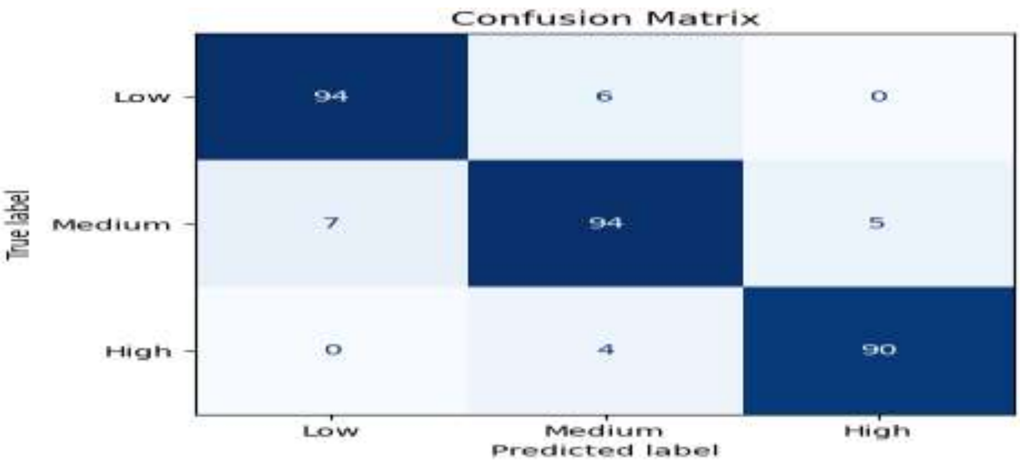

Figure 12 : Confusion Matrix in Scenario 2

5. Conclusion

In this research, a machine learning-based approach was presented for the analysis of solar power generation. In order to calculate the power generated with a fixed irradiance of 1000 and a variable one of 200 to 1000, it uses environmental data.

Above all, our approach exceeded expectations by providing significant findings that contributed to the comprehension of solar power analysis. The confusion matrix obtained a high rate of true positive scenarios almost 80% among all the predictions. And a ROC AUC close to 1 in all the two scenarios.

6. References

1. Huang, Chiou Jye, and Ping Huan Kuo. 2019. “Multiple-Input Deep Convolutional Neural Network

Model for Short-Term Photovoltaic Power Forecasting.” IEEE Access 7:74822–34. https://doi.org/10.1109/ACCESS.2019.2921238.

2. Islam, Sayemul, and Naruttam Kumar Roy. 2023. “Renewables Integration into Power Systems through Intelligent Techniques: Implementation Procedures, Key Features, and Performance Evaluation.” Energy Reports. Elsevier Ltd. https://doi.org/10.1016/j.egyr.2023.05.063.

3. Iweh, Chu Donatus, Samuel Gyamfi, Emmanuel Tanyi, and Eric Effah-Donyina. 2024. “Assessment of the Optimum Location and Hosting Capacity of Distributed Solar PV in the Southern Interconnected Grid (SIG) of Cameroon.” International Journal of Sustainable Energy 43 (1). https://doi.org/10.1080/14786451.2023.2168002.

4. Jang, Jiyeon, Beopsoo Kim, and Insu Kim. 2024. “Comparative Analysis of Deep Learning Techniques for Load Forecasting in Power Systems Using Single-Layer and Hybrid Models.” International Transactions on Electrical Energy Systems 2024 (1). https://doi.org/10.1155/2024/5587728.

5. Jeong, Jaeik, and Hongseok Kim. 2019. “Multi-Site Photovoltaic Forecasting Exploiting Space-Time Convolutional Neural Network.” Energies 12 (23). https://doi.org/10.3390/en12234490.

6. J. Zhu.2001. ‘‘Analysis of Transmission System Faults in The Phase Domain”

7. J. Whatley. 2021. ‘‘Fault Analysis Using Learning Models with Model Interpretation”

8. M. Dimish. 2017.``Fault Detection and Performance Analysis of Photovoltaic Installation”.

9. M. Musaruddin. 2011. ‘‘Automatic Fault Analysis in Power Systems via Application Service Provider”

10. Parlak, Koray Şener. 2023. “A New High Performance MPPT Method Using Only DC-DC Converter in Partial Shade Conditions.” Advances in Electrical and Computer Engineering 23 (3): 75–84. https://doi.org/10.4316/AECE.2023.03009.

11. Sáez, Doris, Fernand Ávila, Daniel Olivares, Claudio Cañizares, and Luis Marín. 2015. “Fuzzy Prediction Interval Models for Forecasting Renewable Resources and Loads in Microgrids.” IEEE Transactions on Smart Grid 6 (2): 548–56. https://doi.org/10.1109/TSG.2014.2377178.

12. Silva, Davi Guimarães da, and Anderson Alvarenga de Moura Meneses. 2023. “Comparing Long Short-Term Memory (LSTM) and Bidirectional LSTM Deep Neural Networks for Power Consumption Prediction.” Energy Reports 10 (November):3315–34. https://doi.org/10.1016/j.egyr.2023.09.175.

13. Supsermpol, Pornpawee, and Navee Chiadamrong. 2023. “Reverse Logistics Network Design with a 3-Phase Interactive Intuitionistic Fuzzy Goal Programming Approach: A Case Study of Covid-19 in Pathum Thani, Thailand.” Engineering Journal 27 (7): 27–51. https://doi.org/10.4186/ej.2023.27.7.27.

14. Tsioumpri, Eleni. 2020. “Fault Anticipation in Distribution Networks PhD Thesis.”

15. Yen, Chih Ta, and Un Hung Chen. 2024. “Design of Deep Learning Acoustic Sonar Receiver with Temporal/Spatial Underwater Channel Feature Extraction Capability.” International Journal of Engineering and Technology Innovation 14 (2): 115–36. https://doi.org/10.46604/ijeti.2023.13057.